Oxygen Distribution and Consumption in the Cat Retina during Normoxia and Hypoxemia

ROBERT A. LINSENMEIER and ROD D. BRAUN

From the Departments of Biomedical Engineering, Neurobiology and Physiology, and Chemical Engineering, Northwestern University, Evanston, Illinois 60208-3107

ABSTRACT Oxygen tension (P_{O_2}) was measured with microelectrodes within the retina of anesthetized cats during normoxia and hypoxemia (i.e., systemic hypoxia), and photoreceptor oxygen consumption was determined by fitting P_{O_2} measurements to a model of steady-state oxygen diffusion and consumption. Choroidal P_{O_2} fell linearly during hypoxemia, about 0.64 mmHg/mmHg decrease in arterial P_{O_2} (P_aO_2). The choroidal circulation provided ~91% of the photoreceptors' oxygen supply under dark-adapted conditions during both normoxia and hypoxemia. In light adaptation the choroid supplied all of the oxygen during normoxia, but at P_aO_2's <60 mmHg the retinal circulation supplied ~10% of the oxygen. In the dark-adapted retina the decrease in choroidal P_{O_2} caused a large decrease in photoreceptor oxygen consumption, from ~5.1 ml O_2/100 g·min during normoxia to 2.6 ml O_2/100 g·min at a P_aO_2 of 50 mmHg. When the retina was adapted to a rod saturating background, normoxic oxygen consumption was ~33% of the dark-adapted value, and hypoxemia caused almost no change in oxygen consumption. This difference in metabolic effects of hypoxemia in light and dark explains why the standing potential of the eye and retinal extracellular potassium concentration were previously found to be more affected by hypoxemia in darkness. Frequency histograms of intraretinal P_{O_2} were used to characterize the oxygenation of the vascularized inner half of the retina, where the oxygen distribution is heterogeneous and simple diffusion models cannot be used. Inner retinal P_{O_2} during normoxia was relatively low: 18 ± 12 mmHg (mean and SD; n = 8,328 values from 36 profiles) in dark adaptation, and significantly lower, 13 ± 6 mmHg (n = 4,349 values from 19 profiles) in light adaptation. Even in the dark-adapted retina, 30% of the values were <10 mmHg. The mean P_{O_2} in the inner (i.e., proximal) half of the retina was well regulated during hypoxemia. In dark adaptation it was significantly reduced only at P_aO_2's <45 mmHg, and it was reduced less at these P_aO_2's in light adaptation.

INTRODUCTION

In cats, hypoxemia (i.e., systemic hypoxia) leads to changes in the standing potential of the eye and in slow components of the electroretinogram (ERG) when arterial

Address reprint requests to Dr. Robert A. Linsenmeier, Biomedical Engineering Department, Northwestern University, 2145 Sheridan Rd., Evanston, IL 60208-3107.

J. GEN. PHYSIOL. © The Rockefeller University Press · 0022-1295/92/02/0177/21 $2.00
Volume 99 February 1992 177–197

oxygen tension (P_aO_2) is as high as 60–70 mmHg (Niemeyer et al., 1982; Linsenmeier et al., 1983). Those components that have been measured in humans appear to be similarly sensitive to hypoxemia (e.g., Marmor et al., 1985; Linsenmeier et al., 1987). The components of the ERG that are altered in mild hypoxemia all originate as changes in membrane potential of retinal pigment epithelial (RPE) cells (Linsenmeier and Steinberg, 1986), but RPE cells, which are adjacent to a rich blood supply, are probably not themselves the site of the sensitivity to hypoxemia. Instead, hypoxemia apparently acts on the photoreceptors, altering the ionic environment around both the photoreceptors and the RPE cells, and causing changes in RPE membrane responses (Linsenmeier and Steinberg, 1984, 1986). Measurements of the oxygen distribution in the normoxic cat retina (Linsenmeier, 1986) suggested that the photoreceptors might be very sensitive to hypoxemia, because the P_{O_2} around the metabolically active part of the photoreceptors was normally nearly zero under dark-adapted conditions, leaving no reserve of oxygen that could be used during hypoxemia. The major purposes of this work were to measure the extent of changes in oxygen availability to the photoreceptors during hypoxemia and quantify the consequent changes in photoreceptor oxygen consumption.

The experiments described here are closely related to recent work in which oxygen distribution and consumption have been studied at increased intraocular pressure (Yancey and Linsenmeier, 1989). This study allows a comparison of hypoxemia with pressure elevation, one of which causes tissue hypoxia by a reduction in P_aO_2, and one of which reduces retinal oxygenation by a reduction in blood flow. The retinal effect that is common to these two situations is a reduction in P_{O_2} in the choroidal circulation behind the retina, but they may be different in other respects. Thus, it is useful to compare the two situations. The work presented here also goes beyond the work on elevated pressure in two ways. First, measurements have been made here in the light-adapted as well as in the dark-adapted retina. This is because hypoxemia is known to have smaller electrophysiological effects in light adaptation (Linsenmeier and Steinberg, 1984, 1986). We have predicted that this is due to a greater oxygen reserve during light adaptation, when photoreceptor metabolism is reduced (Linsenmeier, 1986; Haugh et al., 1990), but experimental evidence of this has not previously been available. Second, an attempt was made here to quantify the status of oxygen supply in the vascularized inner half of the retina, a tissue more similar to other parts of the central nervous system than the outer retina, during normoxia and hypoxemia.

METHODS

Animal Preparation and Recording

The methods used in this work were identical to those described previously (Linsenmeier, 1986; Yancey and Linsenmeier, 1989). Briefly, adult cats were anesthetized with sodium thiamylal during surgery and urethane (200 mg/kg loading dose; 100–200 mg/h maintenance) during recordings. Animals were paralyzed with pancuronium bromide (0.2–0.3 mg/kg·h) and artificially ventilated during recordings to prevent eye movements and to eliminate respiratory compensation during changes of inspired P_{O_2}. Stability of heart rate and femoral arterial pressure were monitored continuously as an indication of the level of anesthesia. It should be

noted that in similarly prepared cats, without muscle relaxation, lower doses of urethane have sufficed for light anesthesia (Enroth-Cugell and Pinto, 1970).

Double-barreled microelectrodes were used, in which one barrel contained a recessed oxygen cathode and the other contained saline for voltage recording (e.g., Linsenmeier and Yancey, 1987). Electrodes were polarized at −0.7 V and were calibrated in vitro at 37°C in a saline-filled chamber through which gases containing 4, 8, and 21% O_2 were bubbled alternately. Current was recorded with a picoammeter (model 614; Keithley Instruments, Inc., Cleveland, OH) and stored on FM tape for later analysis. Electrodes were introduced into the intact right eye through a 15-gauge hypodermic needle. The electrode was sealed in with a boot that prevented leakage of vitreous humor but allowed advancement of the electrode with a hydraulic microdrive. All recordings were made in or near the area centralis.

P_aO_2, P_aCO_2, and pH_a were measured with a blood gas analyzer (model 158; Corning Medical and Scientific, Medfield, MA). During normoxia, the animal breathed air or air supplemented with enough oxygen to keep P_aO_2 generally above 90 mmHg. Under these conditions the arterial values were: P_aO_2, 95.4 ± 14.4 mmHg (mean ± SD); P_aCO_2, 29.0 ± 3.3 mmHg; pH_a, 7.404 ± 0.037 (n = 48 measurements in 14 cats). During hypoxemia, arterial CO_2 and pH were little affected. At P_aO_2's <50 mmHg the values were: P_aO_2, 37.4 ± 9.6 mmHg; P_aCO_2, 29.1 ± 4.1 mmHg; pH_a, 7.412 ± 0.055 (n = 19). A side effect of urethane anesthesia is hyperglycemia (Reinert, 1964). Arterial glucose, measured with a Glucometer II (Ames Division, Miles Laboratories Inc., Elkhart, IN), was 235 ± 52 mg/dl (n = 22 samples in 12 cats).

Experiments were done on animals that were initially dark-adapted. Flashes of diffuse white light were presented as the electrode penetrated the retina in order to elicit ERGs that assisted in monitoring the depth of recording. Once the electrode had penetrated the RPE it was withdrawn in steps of 1 μm at 1–2 μm/s all the way to the vitreous humor, generating a profile of Po_2 as a function of depth. Most of the data presented (all of the oxygen consumption data) are from withdrawals of this type. The vitreal surface during withdrawal was taken to be the point at which the b wave of the ERG changed polarity from negative to positive. The electrode was always moved slightly, to a new retinal location, between profiles.

Penetrations were always done in dark adaptation, but in some cases a diffuse white light was turned on ~60 s before the electrode withdrawal, so that the withdrawal could be done during light adaptation. This light had an illumination sufficient to saturate the rod photoreceptors (8.6 log [equivalent quanta (555 nm)/deg^2·s]) and reduced the photoreceptor oxygen consumption maximally (Linsenmeier, 1986). Light- and dark-adapted series were, in general, performed on different cats. Normoxic dark-adapted profiles were recorded in all animals used for light-adapted series, however, to check that the profiles were similar to those in the animals used for dark-adapted series. These profiles were excluded from the analyses so that the data were not unduly weighted by normoxic profiles in cats where no hypoxemic data were recorded.

Normoxic profiles were recorded first in a typical experiment. The animal was then made hypoxemic by replacing some of the inspired air with nitrogen and more profiles were recorded. In some cases the animal was subjected to another degree of hypoxemia before returning to normoxia, and in other cases normoxia was interposed between measurements at each different hypoxemic level. Durations of hypoxemia were generally less than an hour. Choroidal Po_2 changed rapidly at the beginning of hypoxemia, remained stable during hypoxemia, and recovered rapidly after hypoxemia.

Determination of Oxygen Consumption

The oxygen profile in the outer, avascular half of the retina was fitted to a steady-state model of oxygen diffusion (Haugh et al., 1990). This model assumes that oxygen diffuses only in the radial direction (x), and that all oxygen consumption is confined to a single layer of the outer

retina whose boundaries, L_1 and L_2, and oxygen consumption, Q_2 (in milliliters O_2/100 g tissue·min), are determined by fitting oxygen tension data to the model. This layer typically occupies ~10% of the retinal thickness and corresponds to the location of the mitochondria in the photoreceptor inner segments, within the limits of distortion due to the measurement technique (Haugh et al., 1990). The layers on either side of the consuming layer are assumed to have insignificant oxygen consumption compared with the highly consuming layer. These considerations lead to the model equations:

$$d^2P/dx^2 = 0 \quad 0 < x < L_1$$

$$d^2P/dx^2 = Q_2/Dk \quad L_1 < x < L_2$$

$$d^2P/dx^2 = 0 \quad L_2 < x < L$$

which are solved subject to the boundary conditions that both P (i.e., Po_2) and oxygen flux (Dk dP/dx) must be equal at the boundary between two adjacent layers. Oxygen diffusion coefficient (D) and oxygen solubility (k) were assumed to be the same in all layers. The five parameters of the model were then the Po_2's at the choroid ($P(0) = P_C$) and at the assumed inner edge of the avascular layer ($P(L) = P_L$), which was taken to be halfway through the retina, the boundaries of the consuming region near the choroid (L_1), and near the inner retina (L_2), and the oxygen consumption of the consuming layer divided by its oxygen diffusion coefficient and oxygen solubility (Q_2/Dk). P_C and P_L were strongly constrained by the data, and only the other three parameters were truly unknown. The fitted and measured values of choroidal Po_2 were very similar (slope of the relation between fitted and measured = 1.03; $r = 0.993$), but for consistency the P_C is used only to refer to the fitted parameter and the term "choroidal Po_2" is used otherwise.

Oxygen profiles were measured at an angle of ~45° to the retinal surface, so apparent values of x were multiplied by sin 45° to give actual radial position. It should be noted that $x = 0$ in the model is at the RPE, while the usual conventions of designating the vitreal border of the retina as 0% retinal depth and the RPE as 100% retinal depth are adopted in discussing the results.

The fitting procedure was slightly different than in previous work (Haugh et al., 1990), since it proved possible to reduce the equations to be solved to only two nonlinear equations in L_1 and L_2. This allowed us to generate an error surface that could be easily plotted, allowing us to avoid local minima, and giving confidence in the uniqueness of the fits. The fitting minimized the RMS error between the model and the data, where RMS error = $[[\Sigma\ (Y_i - y_i)^2]^{1/2}]/n$, and n is the number of data values in a profile, Y_i is a data value (i.e., Po_2), and y_i is the ordinate value of the curve at the same abscissa value.

The figures show values of Q_2 and Q_{av} (where $Q_{av} = Q_2\ (L_2 - L_1)/L$ as discussed in the Results), which are more useful than the parameter derived directly from the modeling, Q_2/Dk. To arrive at Q_2, a value has been assumed for D, based on recent measurements in cat retina that indicate a relatively homogeneous value of ~71% of D in saline at 37°C, or 1.97×10^{-5} cm^2/s (Roh et al., 1990). Oxygen solubility has not been measured for retina, and was assumed to be 2.4×10^{-5} ml O_2/ml tissue·mmHg. This is the value for whole blood at 37°C (e.g., Goldstick, 1973), and is approximately an average of the values measured for brain by Thews (1960), Ganfield et al. (1970), and Clark et al. (1978). A correction was also applied to Q_2 (and Q_{av}) to account for the withdrawal distances typically being longer than penetration distances, due to electrode drag. Q_2 values were multiplied by $(2L/D_p)^2$, where D_p is the average retinal thickness measured during all penetrations preceding dark-adapted withdrawals (207 ± 44 μm; $n = 64$ profiles) or all penetrations preceding light-adapted withdrawals (272 ± 44 μm; $n = 46$ profiles). The rationale for this correction arises from the solution to the diffusion equations, and is discussed by Yancey and Linsenmeier (1989).

Unless otherwise indicated, statistics are given as mean ± standard deviation. A P value less than 0.05 on a two-tailed t test was considered significant.

RESULTS

Oxygen Profiles and Oxygen Tension in the Outer Retina

Fig. 1 shows oxygen profiles recorded from one dark-adapted retina during normoxia and at two levels of hypoxemia, illustrating the type of data on which quantitative comparisons are based. The photoreceptors occupy the avascular region, from ~50 to 100% depth from the vitreous. They clearly receive most of their oxygen from the choroid, which is at 100% depth. In all cats the Po_2 decreased to very nearly

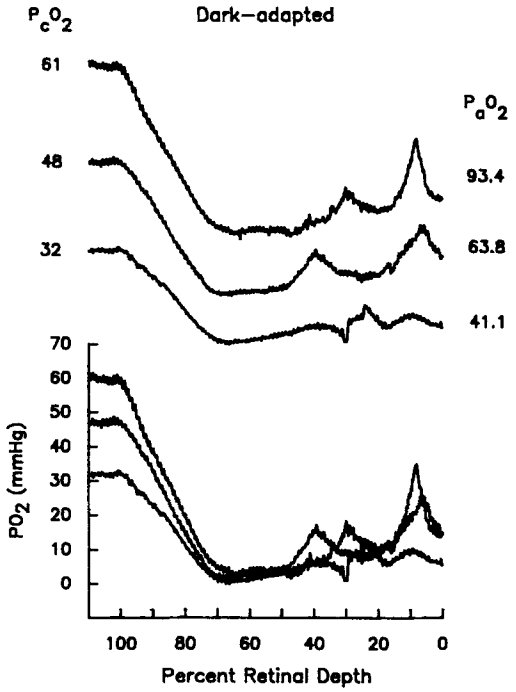

FIGURE 1. Profiles of oxygen tension recorded in one dark-adapted retina during normoxia and hypoxemia. The arterial Po_2 is shown at the right of each trace and the choroidal Po_2 is shown at the left. These are superimposed on an absolute Po_2 scale at the bottom. (Cat 60.)

zero even during normoxia as reported previously (Linsenmeier, 1986; Yancey and Linsenmeier, 1989). In dark-adapted profiles the minimum Po_2 occurred in the oxygen-consuming layer, which lay between 65 and 80% retinal depth in Fig. 1 as defined by the fits to the diffusion model. In the top two profiles the Po_2 remained very low from ~50 to 65% retinal depth, indicating that there was very little diffusion from the retinal circulation to the photoreceptor inner segments, but in the bottom profile and in profiles recorded in other cats there was a more pronounced supply from the retinal side, so that the region having an extremely low Po_2 was smaller. During hypoxemia there was a decrease in choroidal Po_2. There also tended to be a decrease in the slope of the gradient between the choroid and the point of minimum Po_2 that is consistent with the decrease in oxygen consumption discussed below, but

this gradient itself cannot be taken as a measure of consumption, since the other parameters that determine consumption vary between profiles.

In the proximal retina, from 0 to 50% retinal depth, peaks in P_{O_2} were usually observed, presumably reflecting the presence of the capillaries and other small vessels of the retinal circulation. The P_{O_2} distribution in the vascularized part of the retina is discussed separately below.

Examples of oxygen profiles recorded in the light-adapted retina are shown in Fig. 2. Since photoreceptor oxygen consumption is reduced by steady illumination (e.g., Zuckerman and Weiter, 1980; Linsenmeier, 1986), the P_{O_2} decreased more gradually from the choroid to the photoreceptor nuclei. In normoxia all of the oxygen required

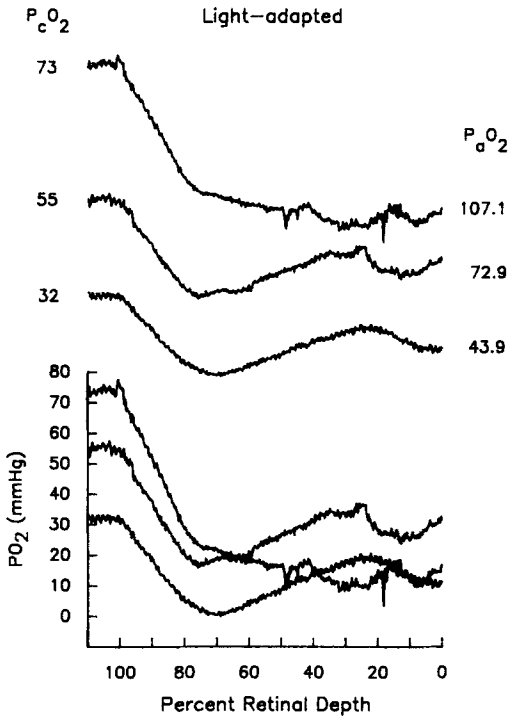

FIGURE 2. Profiles of oxygen tension in one light-adapted retina during normoxia and hypoxemia. The format is as in Fig. 1. (Cat 72.)

by the photoreceptors was supplied by the choroid. The oxygen consuming region is particularly evident as the region near the bend in the normoxic profile at the top (74–81% retinal depth according to the fit to this profile). During hypoxemia choroidal P_{O_2} decreased, just as in dark adaptation, but P_{O_2} remained above zero throughout the outer retina until a relatively severe level of hypoxemia was reached, at a P_aO_2 of 44 mmHg in the example shown. During hypoxemia, oxygen was supplied to the photoreceptors by the retinal as well as choroidal circulations.

The relationship between P_C, the fitted value of choroidal P_{O_2}, and P_aO_2 for 60 dark-adapted and 47 light-adapted profiles is shown in Fig. 3. Each animal is represented by a separate symbol. The dashed line represents the situation where choroidal P_{O_2} equals P_aO_2 and the solid line is a linear regression of all the data

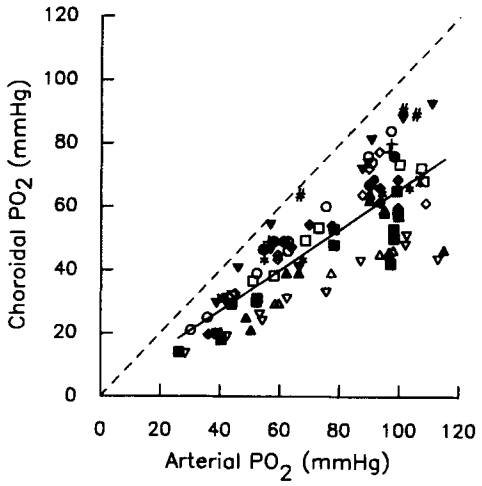

FIGURE 3. Choroidal P_{O_2} as a function of arterial P_{O_2} during normoxia and hypoxemia. The dashed line is the identity line and the solid line is a linear regression of all the data: $P_C = 0.64 \cdot P_aO_2 + 1.66$ ($n = 107$). Each cat is represented here and in subsequent figures by a separate symbol. The open symbols (○, □, △, ▽, and ◇) are data obtained in light-adapted retinas, and the others are from dark-adapted retinas.

($r = 0.80$). Neither the slopes nor intercepts of separate regression lines for dark- and light-adapted data were significantly different. For $P_aO_2 > 85$ mmHg the average value of P_C was 62.2 ± 14.8 mmHg, and 62 is used later as the standard normoxic value of P_C. As shown already by the examples in Figs. 1 and 2, choroidal P_{O_2} decreased with P_aO_2, showing no obvious region of regulation. Choroidal P_{O_2} approached P_aO_2 more closely as P_aO_2 decreased. This is expected from the hemoglobin saturation curve, since equal arteriovenous saturation differences yield smaller arteriovenous P_{O_2} differences at lower values of P_aO_2.

The profiles in Figs. 1 and 2 lead one to expect that the light-evoked increase in P_{O_2} at any point in the outer half of the retina would be smaller in hypoxemia. The profiles provide only an indirect test of this, however, since dark- and light-adapted P_{O_2}'s were measured at different times and in different animals. In five animals measurements of light-evoked changes in P_{O_2} were made before and during hypoxemia while an electrode was positioned in the outer retina. Fig. 4 illustrates the result observed in all cases. In this example the electrode was positioned at 84% retinal depth, where the P_{O_2} in normoxia was nearly zero. During normoxia an increase of

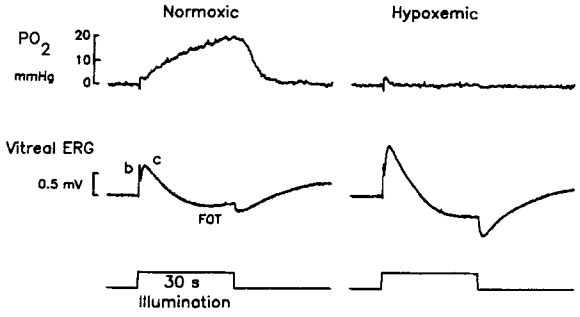

FIGURE 4. Light-evoked changes in outer retinal P_{O_2} during normoxia ($P_aO_2 = 92$ mmHg) and hypoxemia ($P_aO_2 = 49$ mmHg). The top traces show P_{O_2} recorded with an electrode at 84% retinal depth. The initial transient in these records is electrical pickup of the ERG. The middle traces are simultaneously recorded ERGs, showing the b-wave, c-wave, and fast oscillation trough (FOT). The lower trace shows the timing of a 30-s period of illumination at 7.6 log (equivalent quanta [555 nm]/deg^2·s) presented to a dark-adapted retina.

20 mmHg was observed when a light with an illumination about one log unit below rod saturation was turned on for 30 s (top left). 4 min after the onset of hypoxemia (P_aO_2 = 49 mmHg) the same illumination elicited almost no increase in P_{O_2} (top right). The light-evoked increase in P_{O_2} returned to the initial amplitude shortly after the end of the hypoxemic episode (not shown). The middle traces are ERGs recorded simultaneously in the vitreous humor, and show the lack of change in b-wave amplitude, increase in c-wave amplitude, and deepening of the fast oscillation trough expected during hypoxemia (Linsenmeier and Steinberg, 1986).

Photoreceptor Oxygen Consumption

As described in Methods, the outer 50% of each profile was digitized and fitted to a model of oxygen diffusion to determine the oxygen consumption of the photoreceptors and the size of the oxygen consuming layer. The model fitted all the data well, but actually fitted the hypoxemic data slightly better in both light and dark adaptation. This is important, since it allowed the use of the model originally developed for the normoxic case with no modifications. The relation between RMS error (mmHg) and P_C was RMS error = 0.013 (P_C) + 0.53 (n = 112 profiles). The slope was significantly different from zero ($P \ll 0.001$).

Dark adaptation. Values of oxygen consumption (Q_2) derived from 64 profiles in the dark-adapted retina are shown as a function of choroidal P_{O_2} in Fig. 5 *a*. While there is a great deal of scatter in the data, Q_2 decreased during hypoxemia. The correlation coefficient was 0.50 and the slope of the regression line was significantly different from zero ($P \ll 0.001$). The size of the consuming layer as a fraction of the thickness of the whole avascular layer, $(L_2 - L_1)/L$, is shown in Fig. 5 *b*. The thickness of the consuming layer was 20 ± 11% of the thickness of the whole avascular layer (10% of retinal thickness), and was not correlated with choroidal P_{O_2} (r = 0.05). There was no change in the position of the consuming layer (i.e., L_1/L) during hypoxemia (not shown).

At any one choroidal P_{O_2} there was considerable variability among profiles in Q_2 and in $L_2 - L_1$. At least part of this is probably artifactual and results from variable amounts of distortion of the profile caused by the electrode, and from the high sensitivity of the fitted parameters to details of the shape of the profile. One way to partially deal with the variability, and to obtain more meaningful comparisons of Q during normoxia and hypoxemia, is to compute an average oxygen consumption of the avascular layer, $Q_{av} = Q_2 \times (L_2 - L_1)/L$. This is the total oxygen consumption of the avascular layer divided by its thickness. This measure reduces the variability because Q_2 and $L_2 - L_1$ tend to be inversely related to each other (Haugh et al., 1990). A plot of Q_{av} as a function of P_C for the dark-adapted data is shown in Fig. 6. The correlation coefficient is somewhat better than for the data in Fig. 5 *a* (r = 0.67). The solid regression line has a slope of 0.079 ml O_2/100 g tissue·min·mmHg and indicates that halving P_C roughly halves the oxygen consumption, from 5.1 ml O_2/100 g tissue·min at the "normal" P_C of ~62 mmHg to 2.6 ml O_2/100 g tissue·min at a P_C of 31 mmHg. The conclusion is similar if data from each animal are considered separately. The regression lines for each cat are shown in the inset. The slopes of these lines were all positive and had a mean of 0.053 ml O_2/100 g tissue·min·mmHg (±0.034 [SD]; n = 9 cats). The one with the lowest slope is based

on only three points, none of which were at very low P_C. Variation of oxygen consumption as a function of time during hypoxemia was not investigated systematically, but no obvious changes were noted between profiles recorded at the same P_aO_2 but at different times during a hypoxemic episode. The speed of recovery after hypoxemia was not assessed, but Q_{av} had usually recovered by the time the next profile was obtained (~15–30 min).

The dashed line in Fig. 6 is a regression line for similar data obtained during elevation of intraocular pressure (from Fig. 8 of Yancey and Linsenmeier, 1989), and

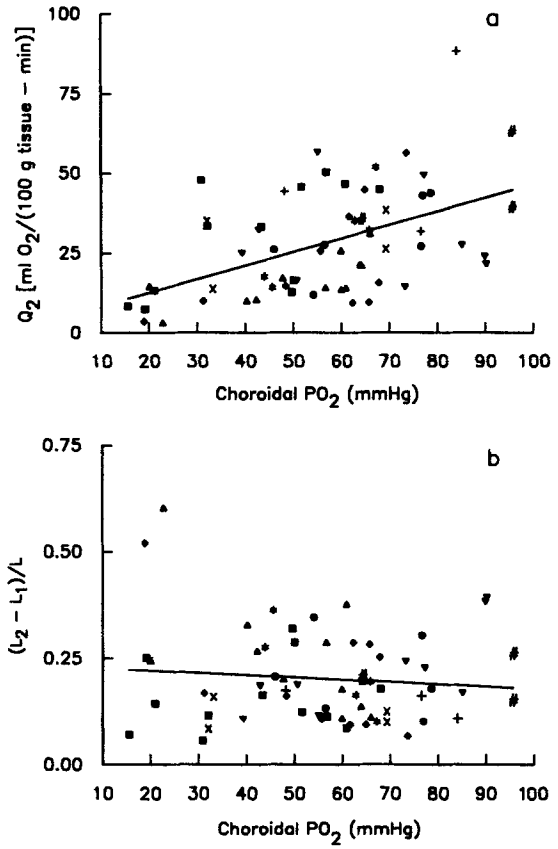

FIGURE 5. Oxygen consumption (Q_2) and relative thickness of the consuming layer $(L_2 - L_1)/L$ in the dark-adapted retina during hypoxemia. Each point was derived from a fit of an oxygen profile to the model described in Methods. The regression line in *a* is: $Q_2 = 0.43 \cdot P_C + 4.19$ ($r = 0.50$; $n = 64$). The regression line in *b* is: $(L_2 - L_1)/L = -0.00053 \cdot P_C + 0.23$ ($r = -0.096$). The slope for $(L_2 - L_1)/L$ vs. P_C was not significantly different from zero.

converted to the units used here. The relationship is similar to that found in hypoxemia.

Some of the oxygen used by the photoreceptors diffuses from the retinal circulation, and to evaluate the importance of this source, the diffusion equations were used to compute the oxygen fluxes into the consuming region through the planes at L_1 (choroidal supply) and L_2 (retinal supply). This requires evaluating the derivative of Eq. 16 of Haugh et al. (1990) at L_1 and L_2, recognizing that the flux into the consuming region at L_1 is positive and at L_2 is negative. The percentage of oxygen

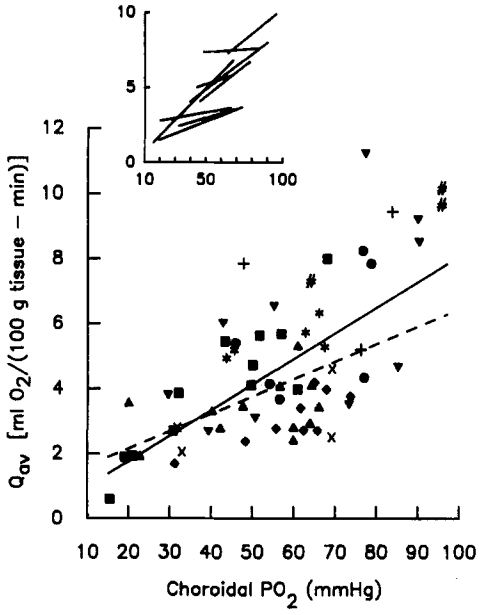

FIGURE 6. Average oxygen consumption (Q_{av}) in the dark-adapted retina during hypoxemia, defined as described in the text. The solid regression line is $Q_{av} = 0.079 \cdot P_C + 0.18$ ($r = 0.67$; $n = 65$). The dashed line is replotted from a study on elevated intraocular pressure (Yancey and Linsenmeier, 1989): $Q_{av} = 0.054 \cdot P_C + 1.08$. One point at $P_C = 29.5$ mmHg included here was omitted from Fig. 5 because the Q_{av} value was reasonable, but Q_2 was very large (593 ml O_2/100 g·min) and $(L_2 - L_1)/L$ was very small (0.007). The inset shows regression lines for each of nine cats and the range of P_C studied in each. The axes are the same as in the main figure.

supplied by the retinal side (Fr) is 100 times the flux through L_2 divided by the total flux, which can be shown to be:

$$Fr = 100[(L_1 + L_2)/2L + (P_L - P_C)/[(Q_{av}/Dk)L^2]]$$

This varied from 0 to ~30% among profiles, averaging 9.4 ± 8.1% ($n = 65$ profiles). Thus, on average, 91% of the oxygen was supplied by the choroid and only 9% by the retinal circulation. The value of Fr did not depend on P_C or P_aO_2.

Light adaptation. Oxygen consumption data for the light-adapted retina are shown in Fig. 7 on the same scale as the data for the dark-adapted retina in Fig. 6. In

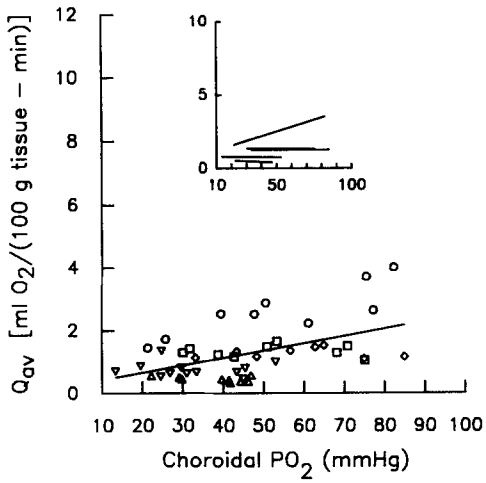

FIGURE 7. Average oxygen consumption (Q_{av}) in the light-adapted retina. The regression line is $Q_{av} = 0.023 \cdot P_C + 0.19$ ($r = 0.51$; $n = 47$). Regression lines for each cat are shown in the inset on the same axes as the main figure.

light adaptation Q_2 and Q_{av} during normoxia were lower than their dark-adapted values. The normoxic Q_{av} during light adaptation (taken from the regression line at P_C = 62 mmHg) was ~1.6 ml O_2/100 g tissue·min, 33% of the corresponding value in dark adaptation. This is lower than the previously reported value of 60%, which was based on a much smaller sample of light-adapted profiles (Haugh et al., 1990). The average normoxic value for Q_{av} is similar to the value that can be calculated by averaging Q over the distal 50% of the retina in Fig. 5 of Alder et al. (1990).

A linear regression of all the data showed some reduction in both Q_2 and Q_{av} during hypoxemia, but the effect of hypoxemia was much less pronounced than during dark adaptation. The slope of the regression line for Q_2 as a function of P_C was not different from zero, and the slope of the regression line for Q_{av} as a function of P_C was 28% of the corresponding slope during dark adaptation. On closer inspection it was clear that for four of the five animals in which light-adapted profiles were measured, there was no change in Q_{av} (i.e., slope not different from zero) down to P_aO_2's of 20–30 mmHg. Only the animal with the highest oxygen consumption during normoxia showed a decrease in Q_{av} during hypoxemia, and this is the reason that the slope in Fig. 7 is not zero. We could find no reason to exclude these data. The size of the oxygen-consuming region, 18 ± 14% (n = 46) of the outer retina, was about the same as in dark adaptation.

During light adaptation the retinal circulation only rarely supplied any oxygen to the photoreceptors when P_aO_2 was >60 mmHg (3 of 29 profiles). At lower P_aO_2, however, the retinal circulation supplied some of the oxygen in 14 of 18 profiles. For these 14 the percentage (Fr) supplied by the retinal circulation was 10.6 ± 9.7%.

Inner Retina

The profiles cannot be used to derive the oxygen consumption of the vascularized part of the retina, because the exact geometry of the vasculature is unknown, and because three-dimensional gradients of Po_2 must exist, but cannot be measured. The extent to which inner retinal Po_2 is regulated during hypoxemia can be determined, however, by making frequency histograms of Po_2 for the inner 50% of the profiles. This technique has been used in many other tissues (e.g., Lübbers, 1977) in which no single value of Po_2 characterizes tissue oxygenation. Histograms of tissue Po_2 in different ranges of P_aO_2 are shown in Fig. 8 for the dark-adapted retina. Each profile contributed ~230 values to these "grand" histograms. A small number of points (0.3%) were excluded because they appeared to represent measurement noise.

A wide range of retinal Po_2 was measured at every P_aO_2, but only part of the range was typically seen in an individual profile. The standard deviation of the normoxic (P_aO_2 > 85 mmHg) histogram compiled from all profiles was 12.6 mmHg, whereas the average standard deviation in 36 histograms prepared from individual profiles was 5.7 mmHg, and only 4 profiles had standard deviations of Po_2 >10 mmHg. Histograms from two representative individual profiles are shown in Fig. 9. Clearly, a penetration through most retinal locations would not yield a range of Po_2's as large as seen in Fig. 8, but the grand histograms represent the overall likelihood of encountering particular values of Po_2 in the inner half of the retina. Corresponding histograms for the light-adapted retina are shown in Fig. 10. In both light and darkness the distributions were positively skewed, as is typical in other tissues

(Lübbers, 1977). The amount of skewness was not large, however, and the median Po_2 was never more than 2.5 mmHg below the mean. Strikingly, even in normoxia in the dark-adapted retina, ~30% of the values were <10 mmHg.

Statistical analysis of inner retinal Po_2 was not performed on the means of the grand histograms, since the number of points was so large that even trivial differences would have appeared statistically different. Instead, the mean Po_2 was

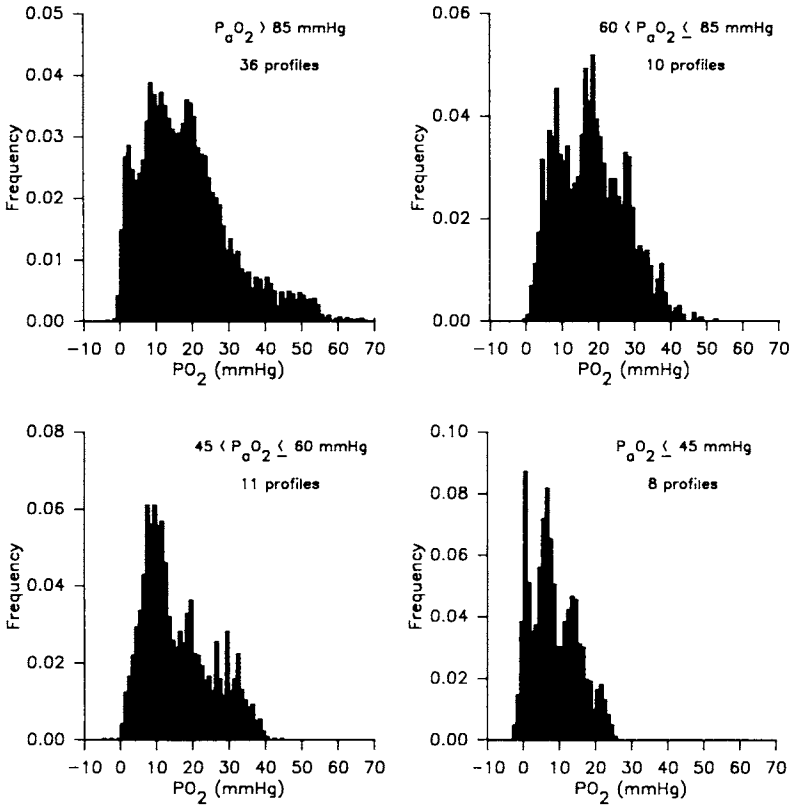

FIGURE 8. Frequency distribution of inner retinal Po_2 in dark adaptation at various ranges of P_aO_2. Absolute frequencies are shown, but the ordinates are scaled so that the histogram shapes can be more easily compared. The number of profiles in each histogram is shown in the figures. The means and standard deviations are: for P_aO_2 > 85 mmHg, 18.4 ± 12.5 mmHg (n = 8,328 values); for 60 < P_aO_2 < 85 mmHg, 18.1 ± 9.4 mmHg (n = 2,312 values); for 45 < P_aO_2 < 60 mmHg, 15.8 ± 9.4 mmHg (n = 2,587 values); for P_aO_2 < 45 mmHg, 8.5 ± 6.4 mmHg (n = 1,822 values).

computed for each profile and then the mean and SEM of the profile means were computed. These are shown graphically in Fig. 11. Table I gives the statistical analysis of these means, which was done with the nonparametric Mann-Whitney test, since at some ranges of P_aO_2 the profile mean Po_2's had a nonnormal distribution (based on normal probability plots). In the dark, the hypoxemic mean Po_2 was different from the normoxic mean Po_2 only when P_aO_2 was <45 mmHg. The

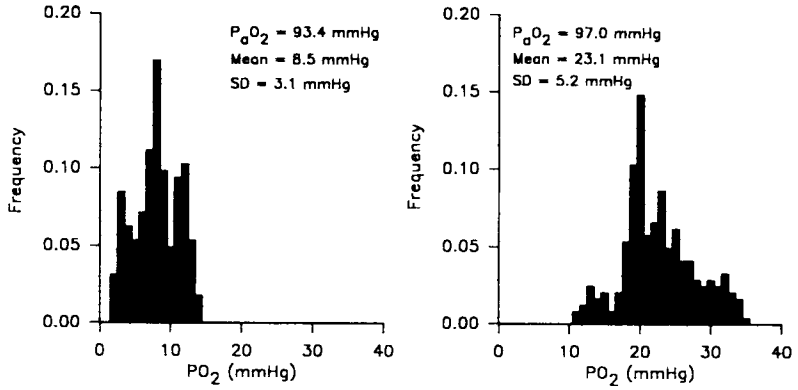

FIGURE 9. Examples of histograms obtained from individual dark-adapted profiles of inner retinal Po_2 during normoxia.

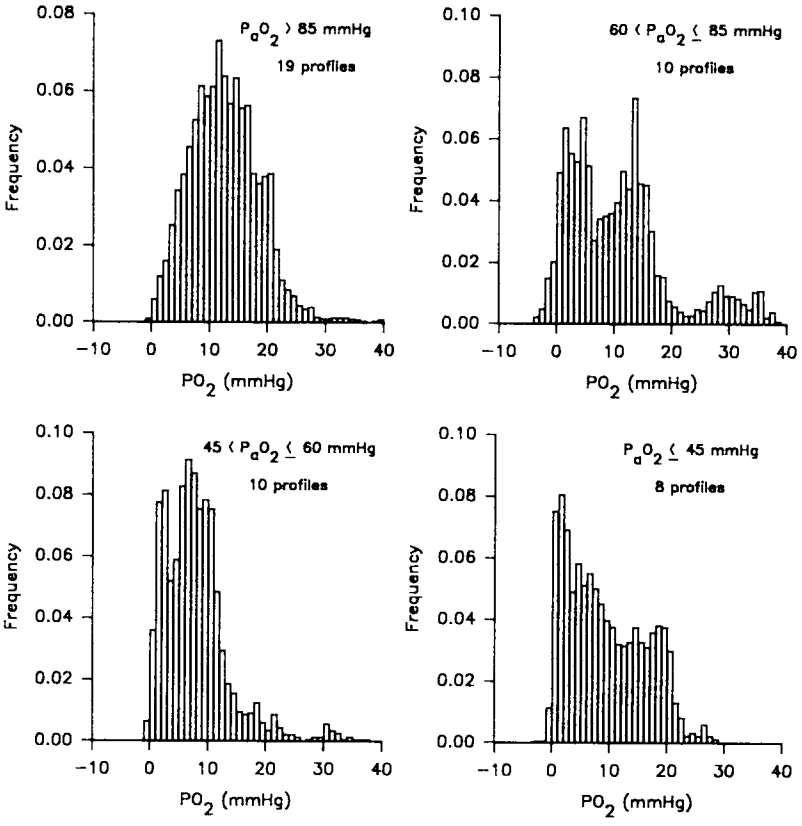

FIGURE 10. Frequency distribution of inner retinal Po_2 in light adaptation at various ranges of P_aO_2. The means and standard deviations are: for P_aO_2 > 85 mmHg, 12.6 ± 5.8 mmHg (n = 4,349 values); for 60 < P_aO_2 < 85 mmHg, 10.7 ± 8.9 mmHg (n = 2,282 values); for 45 < P_aO_2 < 60 mmHg, 7.9 ± 5.7 mmHg (n = 2,310 values); for P_aO_2 < 45 mmHg, 9.3 ± 6.8 mmHg (n = 1,838 values).

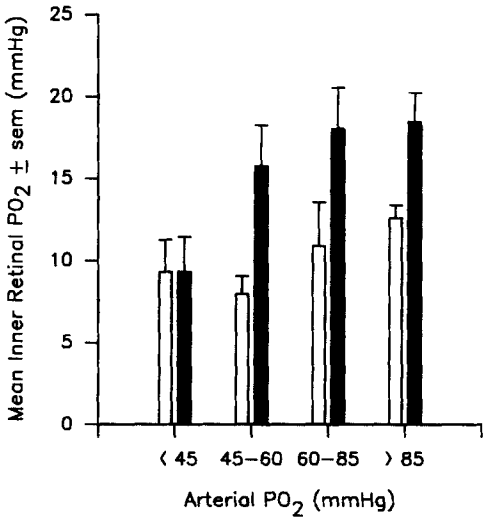

FIGURE 11. Mean inner retinal P_{O_2} (±SEM) during both light adaptation (*open bars*) and dark adaptation (*filled bars*) at four different levels of P_aO_2.

maintenance of inner retinal P_{O_2} is in striking contrast to the linear reduction in choroidal P_{O_2} during hypoxemia (Fig. 3).

During light adaptation the absolute change in inner retinal P_{O_2} was smaller under hypoxemic conditions, and the mean was significantly different from normoxic P_{O_2} only for P_aO_2 in the 45–60 mmHg range. Comparison of dark- and light-adapted P_{O_2} for each range of P_aO_2 (last row of Table I) showed that the means were significantly lower in the light than in the dark during both normoxia and mild hypoxemia.

Since the peaks in P_{O_2} typically appeared to be in the more proximal part of the inner retina, we also examined whether the mean P_{O_2} was higher in the layer from 0 to 25% retinal depth than in the layer from 25 to 50%. This was done with paired *t* tests comparing the mean P_{O_2}'s in each of these layers within each profile. In the dark-adapted retina the P_{O_2} was higher in the more proximal layer for the normoxic profiles (by 4.0 ± 7.5 mmHg; $P = 0.003$) and for the whole sample of profiles (by

TABLE I

P_{O_2} in Inner Retina

	P_aO_2 (mmHg)			
	<45	45–60	60–85	>85
Dark				
Mean of profile				
Means ± SEM	8.5 ± 2.0	15.8 ± 2.5	18.0 ± 2.5	18.5 ± 1.8
n (profiles)	8	11	10	36
P value for hypoxic vs. P_aO_2 > 85	0.005	NS	NS	
Light				
Mean of profile				
Means ± SEM	9.3 ± 2.1	8.0 ± 1.1	10.9 ± 2.7	12.6 ± 0.8
n (profiles)	8	10	10	19
P value for hypoxic vs. P_aO_2 > 85	NS	<0.02	NS	
P value for light vs. dark	NS	<0.02	<0.05	0.028

3.0 ± 6.8 mmHg; $P < 0.001$). This is consistent with the previously reported difference in Po_2 in the two peaks that are usually observed in the inner retina (Yancey and Linsenmeier, 1989). There was no difference in mean Po_2 in the two sublayers of the inner retina for hypoxemic profiles ($P_aO_2 < 85$ mmHg) alone. During light adaptation, no significant differences were found, although the more distal layer tended to have a slightly higher Po_2 during normoxia (by 2.0 ± 4.7 mmHg; $P = 0.08$).

DISCUSSION

The data presented here provide a relatively complete description of intraretinal Po_2 in the cat during hypoxemia, and they are the only such data for any species. Many of the conclusions to be drawn support hypotheses that arose from electrophysiological results and from earlier work on retinal blood flow and vitreal oxygen tension.

Oxygen Consumption

Choroidal Po_2 decreases during hypoxemia because compensatory increases in choroidal blood flow apparently do not occur (Bill, 1962; Friedman and Chandra, 1972). An increase in flow would have a limited effect in any case, since P_aO_2 during relatively mild hypoxemia (60–70 mmHg) falls below the normoxic choroidal venous Po_2, forcing choroidal venous Po_2 to fall. In dark adaptation the decreased choroidal Po_2 decreases the flux of oxygen to the inner segments, since the Po_2 at some point in the inner segment layer was already nearly zero during normoxia. This deficit on the choroidal side is not made up by increased supply to photoreceptors from the retinal circulation (i.e., Fr does not increase during hypoxemia), so the large oxygen demand of the photoreceptors cannot be sustained. In the dark, therefore, Q_{av} decreases by 0.79 ml O_2/100 g tissue·min for a 10 mmHg decrease in choroidal Po_2. Light decreases Q_{av}, which increases outer retinal Po_2. This buffers the photoreceptors against the hypoxemic decrease in choroidal Po_2, and Q_{av} decreases by only 0.23 ml O_2/100 g tissue·min (considerably less in most animals) for the same 10 mmHg change in choroidal Po_2.

Since only one level of illumination was used here, it is reasonable to ask how much light is necessary to protect photoreceptor oxygen consumption from hypoxemia. Certainly the dependence on light is graded, but based on the size of light-evoked changes in Po_2 in the cat retina (Linsenmeier, 1986), it appears that only in the two or three log units below rod saturation would light have a protective effect. At lower illuminations, the Po_2 in the outer retina reaches almost zero during normoxia, and oxygen consumption should therefore be sensitive to hypoxemia not only in dark adaptation, but also over much of the scotopic range.

The decrease in dark-adapted oxygen consumption could conceivably affect many processes in the photoreceptor. Earlier evidence suggested that hypoxemia reduced the activity of the photoreceptor Na^+/K^+ pump, leading to an increase in extracellular $[K^+]$ in the dark and a slowing of the time course of light-evoked changes in $[K^+]$ (Linsenmeier and Steinberg, 1984; Shimazaki and Oakley, 1984). The present results support this, since the reduction in oxygen consumption should lead to a deficit in

ATP production that would be expected to reduce the ion flux through the pump. Whether other cellular processes are also affected is not known. In the light, much smaller increases in extracellular [K^+] were found during hypoxemia (Linsenmeier and Steinberg, 1984). This is consistent with the present finding that much smaller changes in consumption occur, so that ATP production and sodium pumping are less affected.

One objective of this work was to find the relationship of photoreceptor oxygen consumption to P_C in dark adaptation (Fig. 6). We would like to assert that the regression line has physiological significance, that is, that oxygen consumption falls approximately linearly as soon as P_C is reduced. This is consistent with electrophysiological data, particularly the lack of a threshold for the onset of hypoxemic changes in the light peak (Linsenmeier et al., 1983), and with the prediction that when choroidal P_{O_2} falls there is no way to prevent a change in oxygen consumption. A linear relationship of Q_{av} to P_C is not as clear in the data as one might have hoped, however, and it could be argued that over a range of P_C, from ~40 to 70 mmHg, Q_{av} is nearly independent of P_C. Such a plateau may exist, and the relationship may be more complex than expected, but it is at least equally likely that a truly linear relationship between P_C and Q_{av} is somewhat obscured by a combination of measurement error and physiological variation in Q. In this in vivo analysis, oxygen consumption is a highly derived quantity that is subject to error from at least two sources: (*a*) distortion of the profile due to the presence of the relatively large oxygen microelectrode, and (*b*) errors in the calibration of the oxygen electrode. We attempted to deal with the first of these by making the best correction possible for distortion in the apparent length of the profile during withdrawal (see Methods), but this correction is not perfect. The regression line relating Q_{av} to P_C was also recomputed for several types of length correction and after excluding profiles in which L was >25% different from the average L for all profiles in one cat. These made little difference to the slope of the regression line or to the correlation coefficient. Small errors in estimating P_{O_2} from the measured currents are always possible, because even perfectly reproducible in vitro calibrations may not apply exactly in vivo, due to possible changes in temperature or to the diffusion coefficient of the material in the electrode recess. Such errors might add some scatter to the data, but should be in a consistent direction. Another possible source of error is that the model itself is inappropriate. This is unlikely, because (*a*) the model fit well during both normoxia and hypoxemia, (*b*) the model is consistent with the anatomy of the photoreceptors, and (*c*) relative measurements of Q in the retina do not depend very strongly on the choice of the model (Haugh et al., 1990).

While some variation in Q is due to measurement error, there is probably also real physiological variation at a particular value of P_C. Rod density varies by a factor of 1.7 between the center of the area centralis and an eccentricity of 10–15° (Steinberg et al., 1973). This would be expected to influence Q_{av}, but it was not possible to know the rod density at each recording site. It is also possible that in certain regions a greater oxygen supply from the retinal circulation allows a higher Q than would be predicted based on choroidal P_{O_2} alone.

Glycolysis

The retina is known to have a very high glycolytic capacity, which increases under anaerobic or hypoxic conditions (e.g., Graymore, 1959; Winkler, 1986; Yamamoto and Steinberg, 1989), and one can ask whether glycolysis is able to compensate completely for the loss of respiration during hypoxemia. The 36 mol of ATP obtained from 1 mol of glucose during respiration require 6 mol of O_2, so the loss of each mole of O_2 requires that six more moles of ATP be generated glycolytically. The production of these ATP requires the utilization of 3 mol of glucose, replacing the 1 mol of O_2 and 1/6 mol of glucose that had been used in respiration. Therefore, the loss of each oxygen molecule requires three more glucose molecules to be used for glycolysis. As an example, consider the decrease in dark-adapted oxygen consumption (Q_{av}) from 5.1 ml O_2/100 g·min at a normoxic P_C of 62 mmHg to 2.6 ml O_2/100 g·min at a P_C of 30 mmHg (P_aO_2 ~50 mmHg). This is a difference of 0.11 mmol O_2/100 g·min, so 0.33 mmol/100 g·min more glucose would be required to keep ATP production constant. While there have been many measurements of lactate production in the retina, only Törnquist (1979) has measured it in the outer retina of the cat in vivo. From the choroidal arteriovenous difference and choroidal blood flow, the lactate production was found to be 1.91×10^{-4} mmol/min. Assuming that this lactate was generated by glycolysis in the outer half of the retina (wet weight ~65 mg), the normoxic utilization of glucose for glycolysis would be ~0.15 mmol/100 g·min. A similar value was obtained in pig (Törnquist and Alm, 1979). Thus, to completely compensate for the loss of ATP from oxidative metabolism, glycolysis would have to be about three times as great at P_C = 30 mmHg as at P_C = 62 mmHg, utilizing 0.48 vs. 0.15 mmol glucose/100 g·min. Törnquist's value is probably for light adaptation, which is at least somewhat lower than what is expected in dark adaptation (Winkler, 1986; Yamamoto and Steinberg, 1989), so at P_C = 30 mmHg the value might need to be somewhat greater than 0.5 mmol glucose/100 g·min. These values, derived from Q_{av}, assume that glycolysis is spread out over the whole photoreceptor, but to the extent that glycolysis is compartmentalized, the local glycolytic rate would have to be even higher. Such an increase in glycolysis is not out of the question, since anaerobic glucose utilization rates of 0.5 to >0.6 mmol glucose/100 g·min have been reported for whole albino rat retina (Graymore, 1959; Winkler, 1986). The fact that there are effects of mild retinal hypoxemia on electrical signals from the outer retina suggests, however, that glycolytic compensation is not complete, or perhaps that a high rate of glycolysis carries its own detrimental consequences.

Comparison with Intraocular Pressure Elevation

When intraocular pressure was elevated, choroidal Po_2 and oxygen consumption were reduced in the dark-adapted retina (Yancey and Linsenmeier, 1989). Despite other changes, such as acidosis, that probably accompanied the reduction in choroidal blood flow during intraocular pressure elevation, and the blood pressure elevation that sometimes occurs in hypoxemia, the relationship of Q_{av} and P_C was very similar in both cases. Since there was a strong relationship between perfusion pressure (mean arterial pressure minus intraocular pressure) and P_C in the earlier study, and between

P_aO_2 and P_C here, we can give a relationship between the perfusion pressure (PP) and the P_aO_2 that would have equal effects on P_C and therefore on Q. This relationship is:

$$PP = 1.39\ P_aO_2 - 26.3$$

As an example, an arterial Po_2 of 50 mmHg would have the same effect as a PP of 43 mmHg, or for an animal with a mean arterial pressure of 110 mmHg, an intraocular pressure of 67 mmHg.

Inner Retinal Po_2

The average inner retinal Po_2 in dark adaptation is close to 20 mmHg. This value has been based on many measurements and it is similar to previous estimates of inner retinal Po_2 obtained from vitreal and inner retinal measurements in cats and pigs (Alm and Bill, 1972; Tsacopoulos, 1979; Enroth-Cugell et al., 1980; Alder et al., 1983; Linsenmeier, 1986). The wide range of Po_2 observed here was not apparent from the earlier measurements. Mean inner retinal Po_2 decreased during illumination, consistent with changes that sometimes had been observed when Po_2 was recorded at a point in the inner retina during 10–60 s of illumination (Linsenmeier, 1986). It is not known whether the decrease during illumination represents a decrease in blood flow or an increase in oxygen consumption, but the former seems more likely. A decrease in retinal blood flow during illumination has been found in some experiments (e.g., Feke et al., 1983; Bill and Sperber, 1990). The only data directly pertinent to light-induced changes in inner retinal oxygen consumption are deoxyglucose measurements showing no difference in accumulation between darkness and steady illumination (Bill and Sperber, 1990).

Even during dark adaptation inner retinal Po_2 is low compared with tissue Po_2 in most other organs. A survey of Po_2 histograms from various tissues (Kessler, 1974; Leniger-Follert, 1985; Lund, 1985; Schuchhardt, 1985) shows universal agreement that the myocardium has mean Po_2's as low as the inner retina. These are both metabolically active tissues with relatively low venous Po_2's (human retinal venous saturation = 46% [Sebag et al., 1989], corresponding to a venous Po_2 of ~24 mmHg; coronary sinus Po_2 = 20 mmHg [Lund, 1985]). Whether the retina is similar to any other, possibly more heterogeneous, tissues is less clear. Some microelectrode studies in skeletal muscle show low Po_2's (e.g., Heinrich et al., 1985). Mean Po_2's in the range of 15–25 mmHg have also been found in the cerebrum of guinea pig (e.g., Lübbers, 1977) and rat (Feng et al., 1988), but only rarely in cat (Gronczewski and Leniger-Follert, 1984), where the mean is instead generally >30 mmHg (Leniger-Follert, 1985) and there are few values <10 mmHg. Most of the recordings in cat brain have been made with surface electrodes, however, and the Po_2 distribution might be different deeper in the tissue. In cardiac and skeletal muscle, surface electrodes generally give higher values for Po_2 than microelectrodes within the tissue (e.g., Harrison et al., 1990).

Inner retinal Po_2 is well regulated during hypoxemia in both dark and light adaptation, which may be especially important since the values are already low in normoxia. The results reported here support measurements made in the vitreous close to the retina during hypoxemia (e.g., Alm and Bill, 1972; Tsacopoulos, 1979; Enroth-Cugell et al., 1980) in showing that retinal Po_2 is regulated at least as well as

tissue Po_2 in brain, heart, or skeletal muscle (Leniger-Follert et al., 1975; Schuchhart, 1985; Harrison et al., 1990). This regulation is the result of a well-known vasodilation and increase in retinal blood flow during hypoxemia (e.g., Eperon et al., 1975). Regulation of retinal Po_2 is important for maintaining function, since the failure of the ERG b-wave and ganglion cell sensitivity begins when this regulation breaks down at $P_aO_2 < 40$ mmHg (e.g., Linsenmeier, 1990). As noted earlier, photoreceptor metabolism and some ERG components are affected by hypoxemia at considerably higher P_aO_2. This raises the question of how the inner retina manages to preserve function under these conditions, and this requires further study.

We thank Dr. C. M. Yancey for help with early experiments and Dr. T. K. Goldstick for useful discussions.

The work was supported by NIH grant EY-05034 and by the Whitaker Foundation.

Original version received 15 July 1991 and accepted version received 21 October 1991.

REFERENCES

Alder, V. A., J. Ben-Nun, and S. J. Cringle. 1990. Po_2 profiles and oxygen consumption in cat retina with an occluded retinal circulation. *Investigative Ophthalmology and Visual Science.* 31:1029–1034.

Alder, V. A., S. Cringle, and S. J. Constable. 1983. The retinal oxygen profile in cats. *Investigative Ophthalmology and Visual Science.* 24:30–36.

Alm, A., and A. Bill. 1972. The oxygen supply to the retina: I. Effects of changes in intraocular and arterial blood pressures, and in arterial Po_2 and Pco_2 on the oxygen tension in the vitreous body of the cat. *Acta Physiologica Scandinavica.* 84:261–274.

Bill, A. 1962. Aspects of physiological and pharmacological regulation of uveal blood flow. *Acta Societatis Medicorum Upsaliensis.* 67:122–132.

Bill, A., and G. O. Sperber. 1990. Control of retinal and choroidal blood flow. *Eye.* 4:319–325.

Clark, D. K., W. Erdmann, J. H. Halsey, and E. Strong. 1978. Oxygen diffusion, conductivity and solubility coefficients in the microarea of the brain. *Advances in Experimental Medicine and Biology.* 94:697–704.

Enroth-Cugell, C., T. K. Goldstick, and R. Linsenmeier. 1980. The contrast sensitivity of cat retinal ganglion cells at reduced oxygen tensions. *Journal of Physiology.* 304:59–81.

Enroth-Cugell, C., and L. P. Pinto 1970. Gallamine triethiodide (Flaxedil) and retinal ganglion cell responses. *Journal of Physiology.* 208:677–689.

Eperon, G., M. Johnson, and N. J. David. 1975. The effect of arterial Po_2 on relative retinal blood flow in monkeys. *Investigative Ophthalmology.* 14:342–352.

Feke, G. T., R. Zuckerman, G. J. Green, and J. J. Weiter. 1983. Response of human retinal blood flow to light and dark. *Investigative Ophthalmology and Visual Science.* 24:136–141.

Feng, Z.-C., E. L. Roberts, T. L. Sick, and M. Rosenthal. 1988. Depth profile of local oxygen tension and blood flow in rat cerebral cortex, white matter and hippocampus. *Brain Research.* 445:280–288.

Friedman, E., and S. R. Chandra. 1972. Choroidal blood flow. III. Effects of oxygen and carbon dioxide. *Archives of Ophthalmology.* 87:70–71.

Ganfield, R. A., P. Nair, and W. J. Whalen. 1970. Mass transfer, storage and utilization of oxygen in cat cerebral cortex. *American Journal of Physiology.* 219:814–821.

Goldstick, T. K. 1973. Oxygen transport. *In* Engineering Principles in Physiology. Vol. II. J. H. U. Brown and D. S. Gann, editors. Academic Press, New York. 257–282.

Graymore, C. N. 1959. Metabolism of the developing retina. I. Aerobic and anaerobic glycolysis. *British Journal of Ophthalmology.* 43:34–39.

Gronczewski, J., and E. Leniger-Follert. 1984. Relationship between microflow, local tissue P_{O_2} and extracellular activities of potassium and hydrogen ions in the cat brain during intraarterial infusion of ammonium acetate. *Advances in Experimental Medicine and Biology.* 169:291–296.

Harrison, D. K., M. Kessler, and S. K. Knauf. 1990. Regulation of capillary blood flow and oxygen supply in skeletal muscle in dogs during hypoxemia. *Journal of Physiology.* 420:431–446.

Haugh, L. M., R. A. Linsenmeier, and T. K. Goldstick. 1990. Mathematical models of the spatial distribution of retinal oxygen tension and consumption, including changes upon illumination. *Annals of Biomedical Engineering.* 18:19–36.

Heinrich, R., H. Schomerus, W. Fleckenstein, W. Grauer, A. Huber, and C. Weiss. 1985. P_{O_2} distribution in resting muscle and pulmonary gas exchange in patients with cirrhosis. *In* Clinical Oxygen Pressure Measurement. A. M. Ehrly, J. Hauss, and R. Huch, editors. Springer-Verlag, Berlin. 88–92.

Kessler, M. 1974. Oxygen supply to tissue in normoxia and in oxygen deficiency. *Microvascular Research.* 8:283–290.

Leniger-Follert, E. 1985. Oxygen supply and microcirculation of the brain cortex. *Advances in Experimental Medicine and Biology.* 191:3–21.

Leniger-Follert, E., D. W. Lübbers, and W. Wrabetz. 1975. Regulation of local tissue P_{O_2} of the brain cortex at different arterial O_2 pressures. *Pflügers Archiv.* 359:81–95.

Linsenmeier, R. A. 1986. Effects of light and darkness on oxygen distribution and consumption in the cat retina. *Journal of General Physiology.* 88:521–542.

Linsenmeier, R. A. 1990. Electrophysiological consequences of retinal hypoxia. *Graefe's Archive for Clinical and Experimental Ophthalmology.* 228:143–150.

Linsenmeier, R. A., A. H. Mines, and R. H. Steinberg. 1983. Effects of hypoxia and hypercapnia on the light peak and electroretinogram of the cat. *Investigative Ophthalmology and Visual Science.* 24:37–46.

Linsenmeier, R. A., V. C. Smith, and J. Pokorny. 1987. The light rise of the electrooculogram during hypoxia. *Clinical Vision Sciences.* 2:111–116.

Linsenmeier, R. A., and R. H. Steinberg. 1984. Effects of hypoxia on potassium homeostasis and pigment epithelial cells in the cat retina. *Journal of General Physiology.* 84:945–970.

Linsenmeier, R. A., and R. H. Steinberg. 1986. Mechanisms of hypoxic effects on the cat DC electroretinogram. *Investigative Ophthalmology and Visual Science.* 27:1385–1394.

Linsenmeier, R. A., and C. M. Yancey. 1987. Improved fabrication of double-barreled recessed cathode oxygen microelectrodes. *Journal of Applied Physiology.* 63:2554–2557.

Lübbers, D. W. 1977. Quantitative measurement and description of oxygen supply to the tissue. *In* Oxygen and Physiological Function. F. F. Jobsis, editor. Professional Information Library, Dallas. 254–276.

Lund, N. 1985. Skeletal and cardiac muscle oxygenation. *Advances in Experimental Medicine and Biology.* 196:37–44.

Marmor, M. F., W. J. Donovan, and D. M. Gaba. 1985. Effects of hypoxia and hyperoxia on the human standing potential. *Documenta Ophthalmologica.* 60:347–352.

Niemeyer, G., K. Nagahara, and E. Demant. 1982. Effects of changes in arterial P_{O_2} and PCO_2 on the electroretinogram in the cat. *Investigative Ophthalmology and Visual Science.* 23:678–683.

Reinert, H. 1964. Urethane hyperglycemia and hypothalamic activation. *Nature.* 204:889–891.

Roh, H.-D., T. K. Goldstick, and R. A. Linsenmeier. 1990. Spatial variation of the local tissue oxygen diffusion coefficient measured in situ in the cat retina and cornea. *Advances in Experimental Medicine and Biology.* 277:127–136.

Schuchhardt, S. 1985. Myocardial oxygen pressure: mirror of oxygen supply. *Advances in Experimental Medicine and Biology.* 196:21–36.

Sebag, J., F. C. Delori, G. T. Feke, and J. J. Weiter. 1989. Effects of optic atrophy on retinal blood flow and oxygen saturation in humans. *Archives of Ophthalmology.* 107:222–226.

Shimazaki, H., and B. Oakley II. 1984. Reaccumulation of $[K^+]_o$ in the toad retina during maintained illumination. *Journal of General Physiology.* 84:475–504.

Steinberg, R. H., M. Reid, and P. L. Lacy. 1973. The distribution of rods and cones in the retina of the cat (Felis domesticus). *Journal of Comparative Neurology.* 148:229–248.

Thews, G. 1960. Ein Verfahren zur Bestimmung des O_2-Diffusionskoeffizienten, der O_2-Leitfähigkeit und des O_2-Löslichkeitskoeffizienten in Gehirngewebe. *Pflügers Archiv.* 271:227–244.

Törnquist, P. 1979. Aspects of retinal nutrition. PhD thesis. University of Uppsala, Uppsala, Sweden. 26 pp.

Törnquist, P., and A. Alm. 1979. Retinal and choroidal contributions to retinal metabolism in vivo: a study in pigs. *Acta Physiologica Scandinavica.* 106:351–357.

Tsacopoulos, M. 1979. Le role des facteurs metaboliques dans la regulation du debit sanguin retinien. *Advances in Ophthalmology.* 39:233–273.

Winkler, B. S. 1986. Buffer dependence of retinal glycolysis and ERG potentials. *Experimental Eye Research.* 42:585–593.

Yamamoto, F., and R. H. Steinberg. 1989. Effects of mild systemic hypoxia on $[H+]_o$ outside rod photoreceptors in cat. *Society for Neuroscience Abstracts.* 15:206. (Abstr.)

Yancey, C. M., and R. A. Linsenmeier. 1989. Oxygen distribution and consumption in the cat retina at increased intraocular pressure. *Investigative Ophthalmology and Visual Science.* 30:600–611.

Zuckerman, R., and J. J. Weiter. 1980. Oxygen transport in the bullfrog retina. *Experimental Eye Research.* 30:117–127.